Characterization of physicochemical properties of feedlot dust ice crystal residuals (ICRs)

Yidi Hou[1], Petrina Hee[1], Nsikanabasi Umo[2], Ottmar Möhler[2] and Naruki Hiranuma[1]

[1]Dept. of Life, Earth and Environmental Sciences, West Texas A&M University (WTAMU), Canyon, TX, USA; [2]Institute of Meteorology and Climate Research, Karlsruhe Institute of Technology (KIT), Karlsruhe, Germany

West Texas A&M

Karlsruher Institut für Technologie

Objectives & Background

- ❖ ***What are the contributions of feedlot dust size and composition to atmospheric ice nucleation?*** important question towards understanding local cloud and precipitation formation (Rodriguez *et al.*, 2020 and references therein).
- ❖ Our previous work using Raman micro-spectroscopy revealed that ambient dust sampled at a commercial feedlot is predominantly composed of brown or black carbon, hydrophobic humic acid, water soluble organics, less soluble fatty acids and those carbonaceous materials mixed with salts and minerals (Hiranuma *et al.*, 2011).
- ❖ Organic acids (i.e., long-chain fatty acids) and heat stable organics are recently found to be acting as an efficient ice-nucleating particle (INP; DeMott *et al.*, 2018; Perkins *et al.*, 2020).
- ❖ However, our knowledge regarding ***what particulate features of feedlot dust trigger immersion freezing in heterogeneous freezing temperatures*** (i.e., size vs. composition) is still lacking.
- ❖ To improve our knowledge, we conducted ***single particle physicochemical analyses*** of different types of feedlot dust simulants and their ***ice crystal residual (ICR)*** samples.

Aerosol Particle & ICR Sampling

- ❖ We have used two different types of feedlot surface materials, namely ***TXD01 and TXD05***, as surrogates for dust particles observed at the downwind location of feedlots in Texas.
- ❖ TXD01 is a composite sample of surface soils from several commercial and experimental cattle feedlots located in West Texas. The other sample (TXD05) originates from a research feedlot in McGregor, TX.
- ❖ Both samples represent a raw surface material composite from feedlot pens, where cattle are fed without antibiotics nor a direct-fed microbial known as a probiotic.
- ❖ All samples were ground, hammer-milled and sieved for < 75 µm in diameter.
- ❖ ***Heat-treated samples*** (i.e., 100 °C oven-dried for approximately 12 hours) of each type were also produced and examined in this study to assess the heat effect on physicochemical properties.
- ❖ Each sample was injected into the ***AIDA*** (Aerosol Interaction and Dynamics in the Atmosphere) chamber (**Fig. 1a**) for a ***simulated adiabatic expansion experiment*** as demonstrated in Hiranuma *et al.* (2016).
- ❖ Subsequently, ICRs of each sample type were extracted and sampled on proper substrates through an ice-selecting pumped counterflow virtual impactor, ***IS-PCVI***, as described in Hiranuma *et al.* (2016).
- ❖ **Table 1** summarizes characteristics of IS-PCVI properties as well as aerosol particle types used in four ICR extraction expansion experiments (more detailed info available upon request).

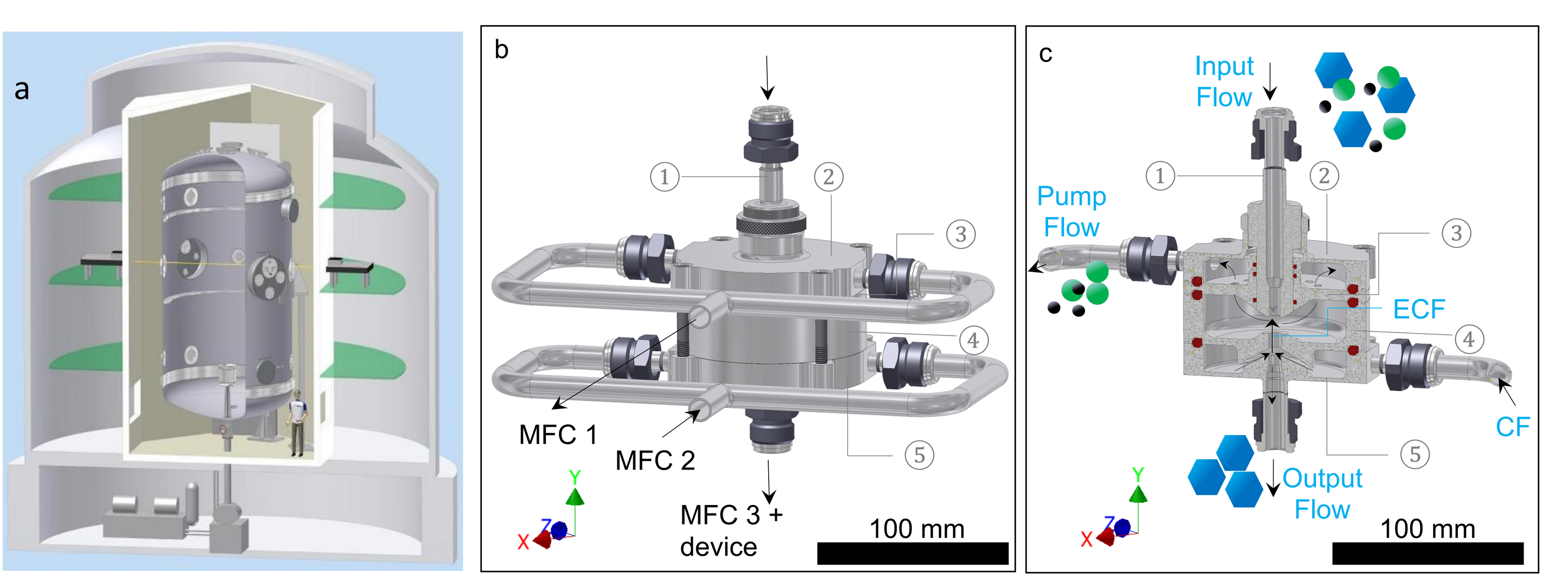

▲ **Figure 1**. Schematic description of the AIDA chamber (a) IS-PCVI outfit (b) and the geometry inside the IS-PCVI (c) – Adapted from Hiranuma *et al.* (2016). The IS-PCVI consists of 5 components: (1) inlet nozzle, (2) top compartment outfitted with the pump flow outlet, (3) rejection plate, (4) middle compartment facilitating the effective counterflow (ECF), and (5) bottom compartment with the counterflow (CF) inlet. The arrows represent the directions of air flows utilized to operate the IS-PCVI.

▼ **Table 1**. Characterization of IS-PCVI properties during the AIDA expansion experiments. The critical cut-size of ice crystals are estimated based on Fig. 9 of Hiranuma *et al.* (2016).

				IS-PCVI properties						
Experiment ID	Reference time (CET)	Aerosol particle type	Simulated cloud type	Input (lpm)	Output (lpm)	ECF (lpm)	CF (lpm)	CF/Input ratio	Pump (lpm)	Critical cut-size, D_c (µm)
TXDUST01_08	10/11/2018 11:30:00	**TXD01**	Mixed-Phase	70.0	2.5	7.0	9.5	0.136	77.0	24.0
TXDUST01_04	10/9/2018 11:11:00	**TXD01_ Dry-Heated**	Mixed-Phase	50.0	2.5	6.5	9.0	0.180	56.5	29.4
TXDUST01_12	10/15/2018 11:14:00	**TXD05**	Mixed-Phase	70.0	2.5	7.0	9.5	0.136	77.0	24.0
TXDUST01_31	10/26/2018 8:38:00	**TXD05_ Dry-Heated**	Mixed-Phase	70.0	2.5	7.0	9.5	0.136	77.0	24.0

Scanning Electron Microscopy (SEM)

- ❖ Our SEM instrument (JEOL JSM-6010LA) is equipped with an Energy Dispersive X-ray spectroscopy (EDX) function with the following optimized parameters used for detections:
  - ➢ Electron beam accelerating voltages of 15 keV
  - ➢ Spot Size (the dimeter of the final beam spot onto the focal point of the sample) of 50
  - ➢ Working Distance (the distance between the objective lens and the focused specimen) of 10mm
- ❖ EDX is a chemical analysis technique used for chemical identification and elemental analysis; it works on the atom's electron transitions and charges interaction to produce the specific and unique X-ray to detect particle compositions.
- ❖ SEM cross-section size analysis was carried out using *Image J*, which is an image-processing tool that can get basic geometry information from any kinds of image formats. We used it to measure particles' diameters horizontally and vertically, then calculate a cross-section average diameter of each particle.
- ❖ Further, EDX can quantify the atomic weight % of a wide variety of elements. The atomic weight percentage can be calculated and converted by the weight % as:
  Atomic % = weight % / Atomic weight

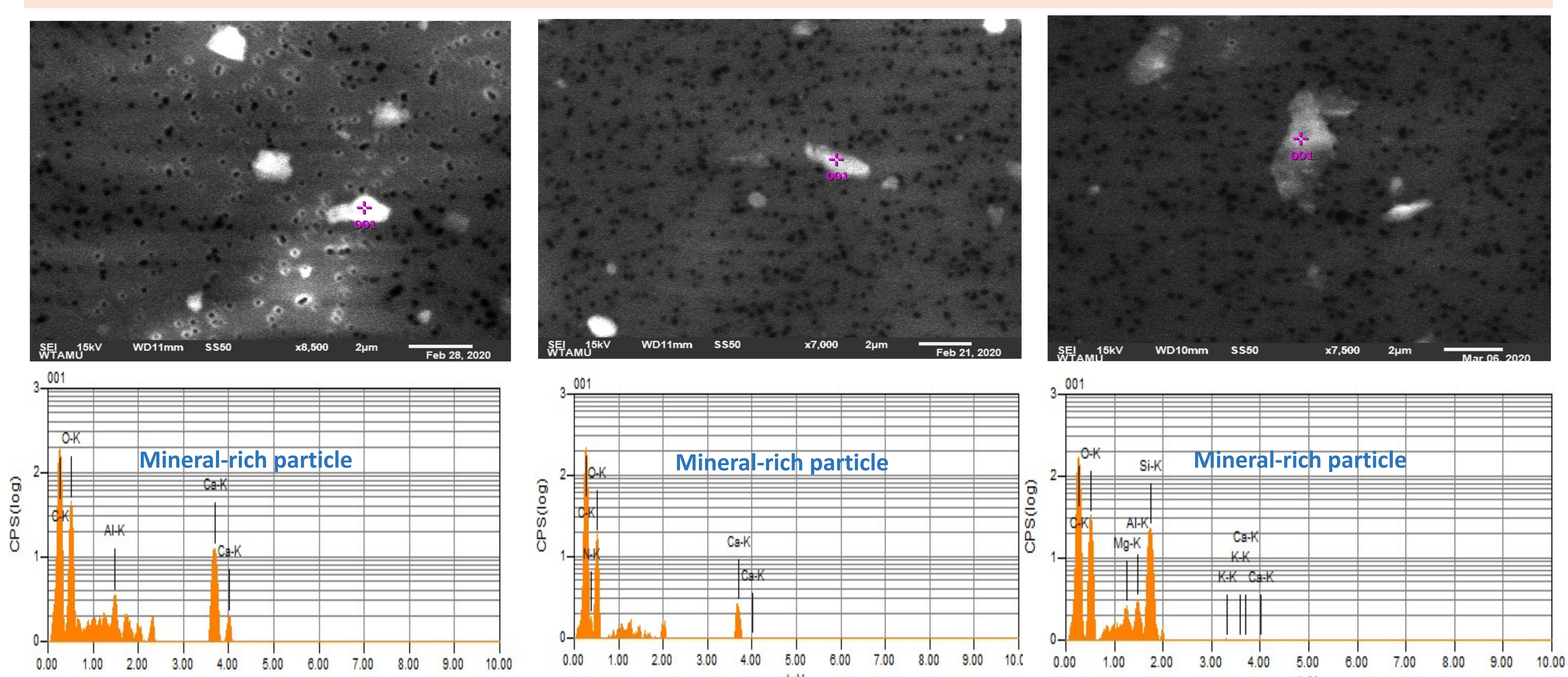

▲ Figure 2. a. Example SEM image and EDX spectrum (k means electron shell) of TXD01 (aerosol particle)(ID:TXD01_11.10.2018_b_003)

▲ Figure 2. b. Example SEM image and EDX spectrum (k means electron shell) of TXD05 (aerosol particle)(ID:TXD05_15.10.2018_b_002)

▲ Figure 2. b. Example SEM image and EDX spectrum (k means electron shell) of TXD01 (dry heated-residuals)(ID:TXD01_H_09.10.2018_003)

Physical Properties

- ❖ A total of 1259 particles in the size range of 0.2 to 3 µm diameter was assessed through SEM.
- ❖ **Table 2 and Fig. 3** summarize size properties of these particles. The number of measured particles was limited depending on the particle availability on each substrate. Nevertheless, we looked into at least 100 particles for each sample type as seen in the table. Out of these particles, the diameter of TXD01 particles was on average smaller than TXD05.
- ❖ Higher aspect ratios in residuals compared to aerosol particles was found for both TXD01 and TXD05 samples. Moreover, the TXD05 and TX D01 dry-heated residuals have higher aspect than non-heated. This difference indicates a relative increase in non-spherical particles in residuals. In short, Hiranuma *et al.* (2008) found quasi-spherical feedlot-emitted particles were predominantly salt rich hygroscopic particles, whereas non-spherical amorphous particles were found to be and organic dominant with negligible hygroscopicity. Our results suggest high non-spherical organic contents in residuals.

Table 2. Summary of particle size properties through electron microscopy.

Sample Type	Measured Particles	*Diameter (µm) Average	*Diameter (µm) Std. Error	**Aspect Ratio Average	**Aspect Ratio Std. Error
TXD01 aerosol	159	0.80	0.03	1.46	0.04
TXD01 residual	185	0.87	0.03	**1.56↑**	0.04
TXD01H dry-heated aerosol	162	0.82	0.03	1.42	0.03
TXD01H dry-heated residual	126	0.90	0.04	**1.48↑**	0.05
TXD01 cumulative	632	**0.84**	0.02	1.48	0.02
TXD05 aerosol	194	0.99	0.03	1.37	0.03
TXD05 residual	164	1.17	0.03	**1.49↑**	0.03
TXD05H dry-heated aerosol	100	1.23	0.04	1.41	0.05
TXD05H dry-heated residual	169	0.90	0.03	**1.49↑**	0.04
TXD05 cumulative	627	**1.05**	0.02	1.44	0.02

*Average of cross sections. **Ratio of cross sections (i.e., longer cross section/shorter cross section).

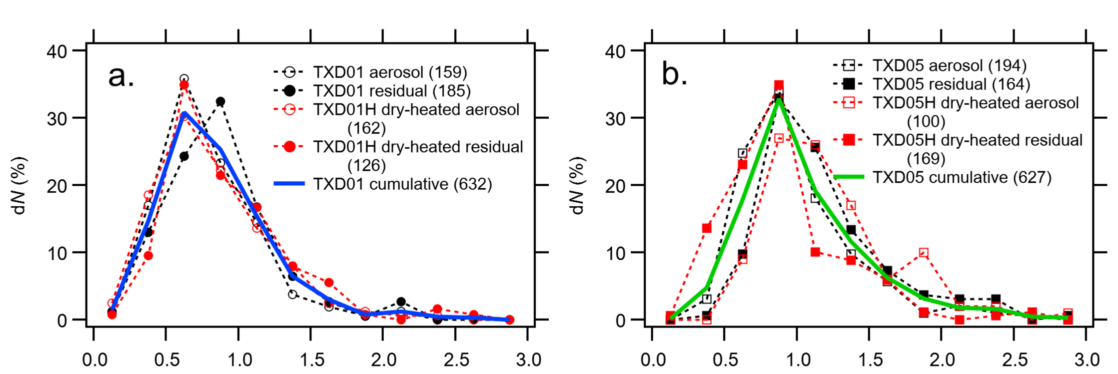

◀ **Figure 3**. Size distributions of aerosol particles (open symbol) and ice crystal residual particles (solid symbol) for TXD01 (a) and TXD05 (b) in normalize *dN* (0.25 µm intervals). A pair of non-heated (black) and dry-heated (red) samples was analyzed for both (a) and (b). The numbers in parentheses represent a total number of particles analyzed for each sample.

Chemical Properties

- ❖ **Table 3 and Fig. 4** show the summary of the elemental compositions (types according to Hiranuma *et al.*, 2013) for samples used in this study. Briefly, an increase in organic fractions as well as a substantial decrease in salt inclusions in residuals persisted for both TXD01 and TXD05 samples. This observation supports the result in **Table 2**. The reduction in salt is relevant to an increase in aspect ratio (Hiranuma *et al.*, 2008). This observation may be also indicative of predominance of immersion freezing (rather than condensation freezing) for residual production (e.g., Hande and Hoose, 2017).
- ❖ As seen in **Fig. 5**, no clear size-dependence of elemental compositions in both total aerosol and residual samples was found.

Table 3. Summary of particle elemental compositions through energy dispersive X-ray spectroscopy.

Particle Type	TXD01 Abundance (%) Aerosol	TXD01 Residual	TXD01 Dry-heated Aerosol	TXD01 Dry-heated Residual	TXD05 Abundance (%) Aerosol	TXD05 Residual	TXD05 Dry-heated Aerosol	TXD05 Dry-heated Residual
Organic (C,N,O)	5.0	**7.6↑**	3.1	**9.5↑**	8.2	**9.1↑**	3.0	**11.2↑**
Salt-rich (Na,Mg,K,P)	34.6	**10.3↓**	35.8	**4.0↓**	22.2	**4.9↓**	15.0	**10.1↓**
Mineral-rich (Al,Si,Ca)	57.2	77.8	56.2	70.6	68.0	82.9	79.0	74.6
Other	3.1	4.3	4.9	15.9	1.5	3.0	3.0	4.1

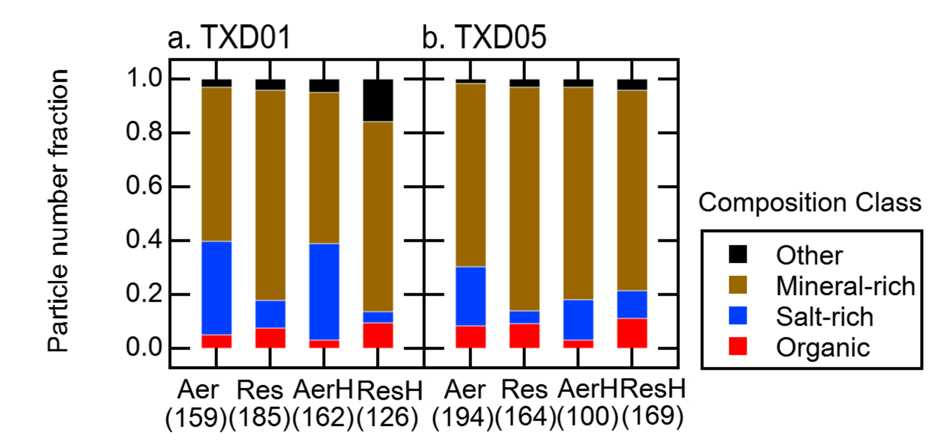

◀ **Figure 4**. Stacked column diagram of particle composition class for the studied particle population, including total aerosol particles (Aer) and ice crystal residuals (Res), for a set of TXD01 samples (a) and TXD05 samples (b). "H" indicate the dry-heated sample. The numbers in parentheses represent a total number of particles analyzed for each sample.

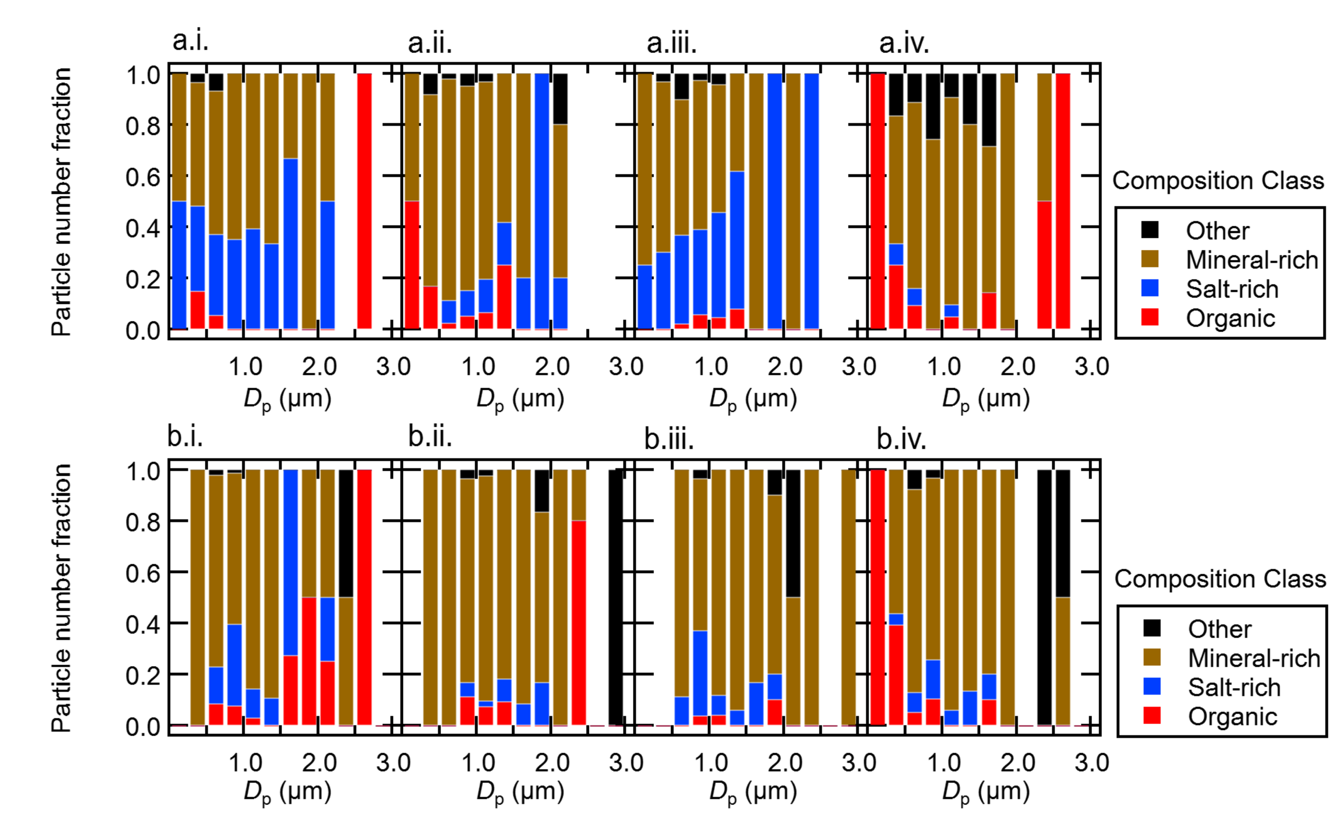

▲ **Figure 5**. Stacked column diagram of particle composition class as a function of particle diameter for the studied particle population for a set of TXD01 samples (a) and TXD05 samples (b). Horizontal panels are ordered for total aerosol particles (i), ice crystal residuals (ii), dry-heated aerosol particles (iii), and dry-heated residual particles (iv).

Summary & Outlook

- ❖ This is consistent with the previous study of TXD particles composition analyses, aerosol particle composition is dominated by organics with substantial inclusion of salts (e.g., potassium). (Hiranuma *et al.*, 2011).
- ❖ The elemental composition analysis revealed some notable difference between aerosol particle samples and residual samples, indicating the inclusion of non-hygroscopic organic particles as ice residuals.
  Our ICR analysis also revealed a decrease in hygroscopic salt inclusion in residuals, which may imply an importance of immersion rather than condensation freezing as agricultural INPs. (INPs directly immerse in a supercooled water and trigger the freezing between 0 °C and −37 °C.)
- ❖ Heat-resistant physicochemical properties and super micron nature of feedlot-emitted INPs also are highlighted this study.
- ❖ Further research should focus on understanding how organic composition and/or other particulate properties influence ice nucleation. Such organic INP dataset has long been a missing piece in the study area of cloud microphysics and atmospheric chemistry and is of importance to improve atmospheric models of cloud feedbacks and determine their impact on the regional weather and climate.
  Besides, We need a trans-Texas feedlot study to look into how cattle diet (antibiotics, probiotics etc.) influences physicochemical properties in aerosol particles and ICRs of feedlot surface materials.

References

DeMott P. J. et al.: Environ. Sci.: Processes Impacts, 20, 1559–1569, 2018.
Hande, L. B. and Hoose, C.: Atmos. Chem. Phys., 17, 14105–14118, 2017.
Hiranuma, N. et al.: Atmos. Environ., 42, 1983–1994, 2008.
Hiranuma, N., et al.: Atmos. Chem. Phys., 11, 8809–8823, 2011.
Hiranuma, N. et al.: J. Geophys. Res. Atmos., 118, 6564–6579, 2013.
Hiranuma, N. et al.: Atmos. Meas. Tech., 9, 3817–3836, 2016.
Perkins, R. J. et al.: ACS Earth Space Chem., 4, 133–141, 2020.
Rodriguez, C. A. et al.: ESSOAr, DOI: https://www.essoar.org/doi/abs/10.1002/essoar.10502568.1, 2020.

Acknowledgement: This material is based upon work supported by the U.S. Department of Energy, Office of Science, Office of Biological and Environmental Research program (DESC0018979, Atmospheric Processes) under Early Career Research Program Award (DE-FOA-0001761). Y. Hou thanks for the funding support from WTAMU President's Undergraduate Student Research Program and WTAMU Engineering Core Lab at PDRF for technical support.